

Molecular and Anatomic Imaging of Neuroendocrine Tumors

Laszlo Szidonya, MD, PhD^{a,b}, Eunkyung Angela Park, MD, PhD^c,
Jennifer J. Kwak, MD^d, Nadine Mallak, MD^{a,*}

KEYWORDS

- Neuroendocrine tumor • Somatostatin receptor • Positron emission tomography
- Imaging • Peptide receptor radionuclide therapy • Appropriate use • Management

KEY POINTS

- Computed tomography and magnetic resonance imaging obtained for a known or suspected neuroendocrine tumor should include multiphase contrast-enhanced imaging of the abdomen.
- ⁶⁴Cu-DOTATATE is considered equivalent to ⁶⁸Ga-labelled agents; it offers logistical advantages of remote production of the radiopharmaceutical and flexible scanning times.
- High-grade neuroendocrine tumors demonstrate FDG uptake, usually with a concomitant decrease in somatostatin receptor expression. FDG uptake is an important negative prognostic factor.
- Changes in standardized uptake values alone on somatostatin receptor positron emission tomography after peptide receptor radionuclide therapy should not be interpreted as disease response or progression. The changes in size on anatomic imaging and appearance or resolution of lesions on somatostatin receptor positron emission tomography should be used instead.

INTRODUCTION

Neuroendocrine neoplasms (NENs) are a diverse group of tumors originating from neuroendocrine cells present throughout the body.¹ These tumors share common morphologic, histologic, and biochemical features; the majority express somatostatin receptors (SSTRs) on the cell surface, which can be used as imaging and therapeutic targets.²

^a Oregon Health & Science University, 3181 Southwest Sam Jackson Park Road, Mail Code L340, Portland, OR 97239, USA; ^b Diagnostic Radiology, Heart and Vascular Center, Semmelweis University, Budapest, Hungary; ^c Division of Nuclear Medicine, Department of Radiology, University of Iowa Hospitals and Clinics, 200 Hawkins Drive, Iowa City, IA 52242, USA; ^d Department of Radiology, School of Medicine, University of Colorado, 12401 East 17th Avenue, Mail Stop L954, Aurora, CO 80045, USA

* Corresponding author.

E-mail address: mallak@ohsu.edu

NENs include the well-differentiated neuroendocrine tumors (NETs) and the poorly differentiated neuroendocrine carcinomas (NECs). These tumors are classified based on their proliferation index (or Ki-67) and mitotic count. The 2010 and 2017 World Health Organization (WHO) classifications are detailed in **Table 1**. The most important change brought by the 2017 classification for pancreatic NETs (PNETs) is further dividing G3 tumors into well-differentiated G3 NETs (Ki-67 > 20%, however, <50%–55% typically) and NECs (high-grade by definition, with poorly differentiated morphology and Ki-67 > 20%, most commonly ≥50%–55%). NECs display more malignant features and biological behavior and include the small-cell and large-cell types.³ In 2018, the International Agency for Research on Cancer and WHO expert consensus proposal expanded the 2017 WHO classification of PNETs to NETs of the gastrointestinal (GI) tract,³ a change that has been reflected in the 2019 WHO classification of tumors of the digestive system.⁴

Anatomic Imaging

NETs are often discovered incidentally on computed tomography (CT) scans performed for other indications. Whenever a CT or a magnetic resonance imaging (MRI) is obtained for a known or suspected NET, it should be performed with multi-phase contrast-enhanced imaging of the abdomen. Most primary PNETs and hepatic metastases are hyperenhancing and better visualized on the arterial phase (**Figs. 1** and **2**); however, due to tumor heterogeneity, even within the same individual, some tumors may be hypoenhancing and better detected on standard portal venous or delayed phases (see **Fig. 2**; **Fig. 3**).^{5–7}

CT detection rate of primary PNETs is high, estimated at 80% to 100%⁸ but it is much lower for primary small bowel NETs, reported to be around 50%.^{5,9}

MRI is superior to CT for the detection of hepatic metastases.^{10,11} Two particularly helpful sequences are diffusion-weighted imaging,¹² and delayed postcontrast phase using hepatospecific contrast agent (or Gadoteric acid), which is considered the most sensitive tool for the detection of hepatic metastases.^{12–14}

Several imaging features on CT and MRI have been associated with a high-tumor grade: large tumor size (>2 cm), ill-defined tumor margins, low arterial hyperenhancement, presence of pancreatic duct dilatation, nonbright T2 signal, and most importantly, high diffusion restriction on MRI.¹⁵

Classification/Grade	2010		2017 (Pancreas, Later Expanded to GI Tract in 2019)	
	Mitotic Rate ^a	Ki-67%	Mitotic Rate ^b	Ki-67%
G1 (Low grade)	<2	<2%	<2	<3%
G2 (Intermediate grade)	2–20	3%–20%	2–20	3%–20%
G3 (High grade)	>20	>20%	Well-differentiated NETs >20	>20%, typically <50%–55%
			Poorly differentiated NECs >20	>20%, typically ≥50%–55%

^a Per 10 HPF.

^b Per 2 mm².

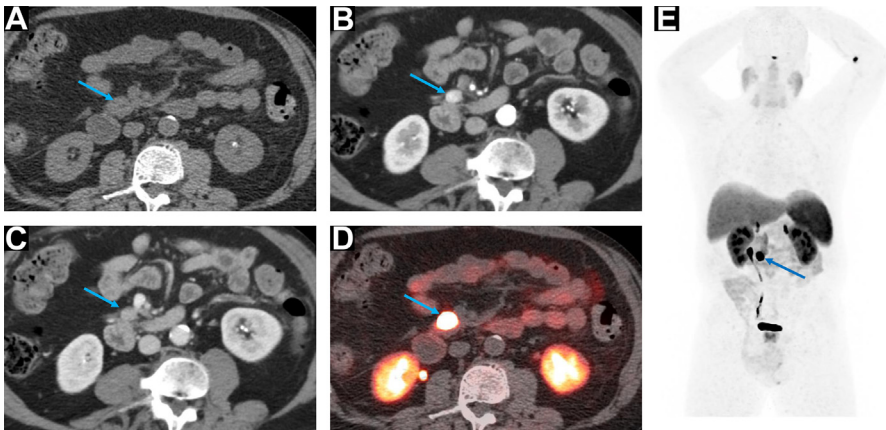


Fig. 1. PNET (arrows) on multiphase contrast-enhanced CT of the abdomen: precontrast (A), arterial (B), and portal venous (C) phases, demonstrating arterial hyperenhancement with subsequent washout. ^{64}Cu -DOTATATE PET/CT axial fused (D) and maximum intensity projection (MIP) (E) images show intense uptake in the lesion and no evidence of metastatic disease.

Functional Imaging with Somatostatin Receptor Positron Emission Tomography Agents

The SSTR expression on most NETs makes functional imaging with SSTR ligands possible.¹⁶

The gamma camera imaging agent ^{111}In -pentetreotide (OctreoScanTM, Curium US LLC, Maryland Heights, MO, USA) was the first Food and Drug Administration (FDA)-approved radiotracer for the functional imaging of NENs in 1994 but it has been replaced by PET imaging agents, which are superior on all levels, as detailed in [Table 2 \(Fig. 4\)](#).¹⁵

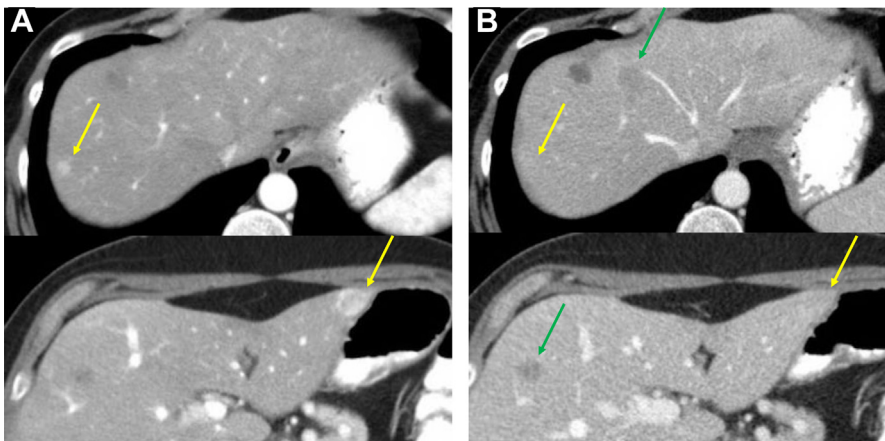


Fig. 2. Hepatic metastases from G2 PNET. Multiphase contrast enhanced CT, arterial (A) and portal venous (B) phases. Some lesions are arterially enhancing and seen only on the arterial phase (yellow arrows), others are hypoenhancing and better visualized on the venous phase (green arrows).

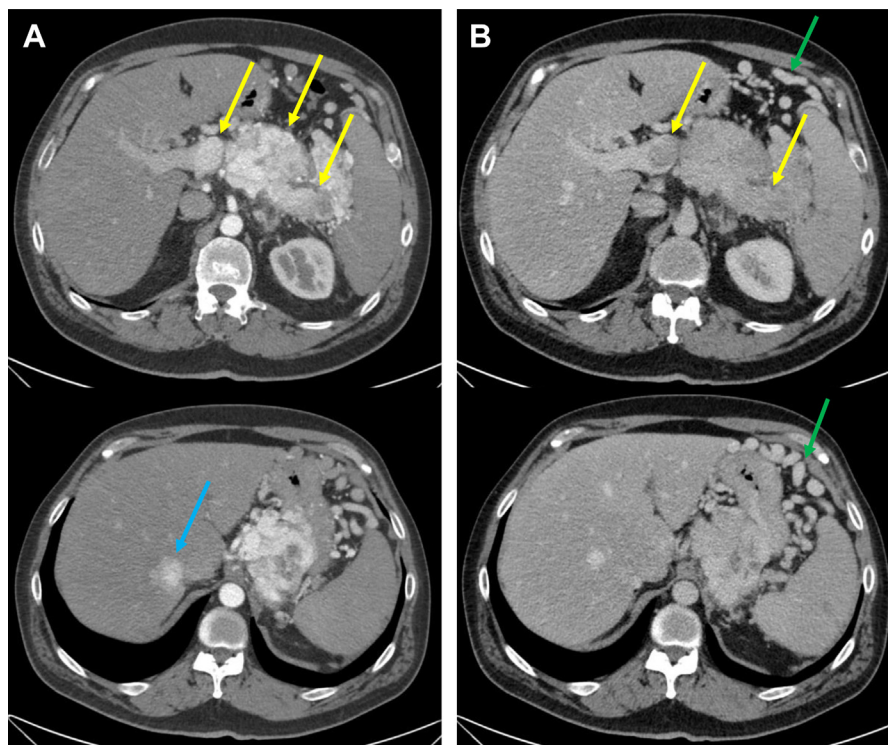


Fig. 3. G3 NET of the pancreatic tail, patient presenting with gastrointestinal bleed. Multi-phase contrast-enhanced CT of the abdomen, arterial (A) and portal venous (B) phases. The mass enhances on the arterial phase, with a tumor thrombus involving the splenic and portal veins (yellow arrows), and collateral veins in the left abdomen (green arrows). Hyperenhancing liver metastasis is seen only on the arterial phase (blue arrow).

Although there are some differences in the relative affinity of the different ^{68}Ga -labelled PET radiotracers to each subtype of SSTRs, they are considered clinically equivalent:

- ^{68}Ga -DOTATATE (NETSPOTTM, Advanced Accelerator Applications USA, Inc. Millburn, NJ 07041): FDA-approved in 2016¹⁷ and commercially available.
- ^{68}Ga -DOTATOC: FDA-approved in 2019¹⁸ but not commercially available.
- ^{68}Ga -DOTANOC: not FDA approved yet.

In 2020, ^{64}Cu -DOTATATE (DetectnetTM, Curium US LLC, Maryland Heights, MO, USA) joined the list of FDA-approved and commercially available PET radiopharmaceuticals¹⁹ (detailed in later discussion).

A multidisciplinary group convened by the Society of Nuclear Medicine and Molecular Imaging (SNMMI) developed appropriate use criteria (AUC) for these agents, published in 2018.²⁰ The most appropriate indications are detailed in **Table 3** (see **Fig. 1**; **Figs. 5–10**).

In November 2020, an update to the AUC was published, adding ^{64}Cu -DOTATATE to the list of accepted SSTR PET radiopharmaceuticals, along with a new appropriate indication, which is the restaging of patients after PRRT.²¹ The update also indicates that the number of SSTR PET scans performed during a patient's lifetime should not

Table 2
Comparison between the commercially available NET imaging agents

	¹¹¹ In-pentetreotide Scan	⁶⁸ Ga-DOTATATE PET	⁶⁴ Cu-DOTATATE PET
Brand name	OctreoScan	NETSPOT	Detectnet
Diagnostic accuracy	Good	Significantly superior to OctreoScan for detection of small lesions (particularly lung and bone)	Slightly more superior to ⁶⁸ Ga agents for detection of small lesions (particularly lymph nodes)
Patient convenience	Two-day protocol (imaging @ 4 and 24 or 24 and 48 h postinjection [p.i.])	One-day protocol (imaging @ 40–90 min p.i.)	One-day protocol with more flexible uptake period (imaging @ 45–180 min p.i.)
Physical T1/2	67.3 h	1.1 h	12.7 h
Injection dose	111/222 MBq (planar/SPECT)	2 MBq/kg, up to 200 MBq	148 MBq
Radiation dose ^a	Higher (13 mSv/111 MBq 26 mSv/222 MBq)	Lower (3.15 mSv/150 MBq)	Lower (4.7 mSv/148 MBq)
Availability	Readily available	Commercially available in most areas but can be limited by ⁶⁸ Ge/ ⁶⁸ Ga generator availability	Commercially available as ready-made vials, can be distributed to centers without cyclotrons

^a Excluding radiation from low-dose CT (CTs of SPECT/CT or PET/CT).

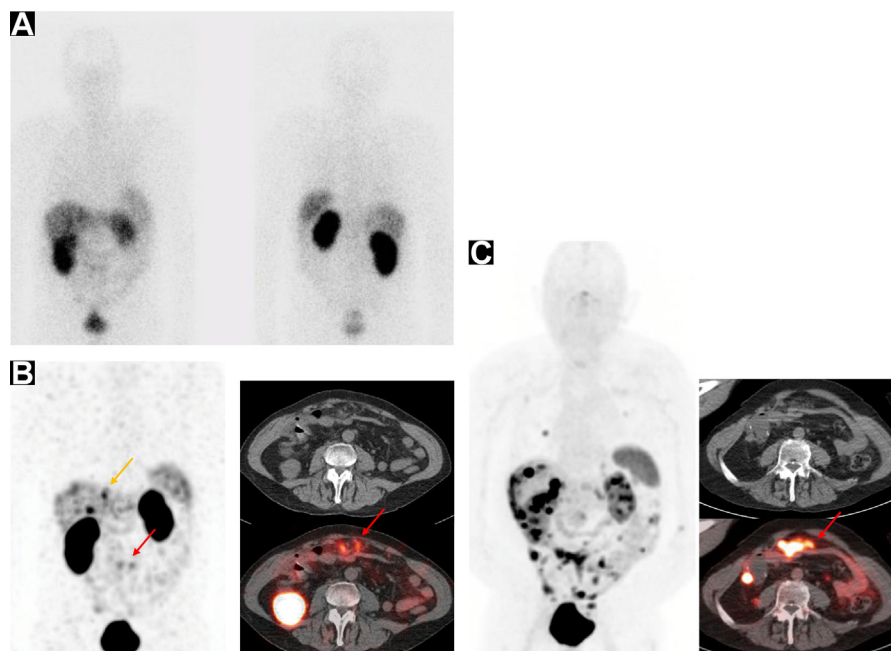


Fig. 4. Patient with resected small bowel NET. Faint liver lesions are seen on OctreoScan planar images (A) at 24 hours, more visible on SPECT/CT (B, yellow arrow), with additional peritoneal disease (red arrows). ^{68}Ga -DOTATATE PET/CT (C) shows much more extensive liver and peritoneal metastases (red arrow) and 2 rib lesions.

be limited, since SSTR PET plays an important role in disease management at various times. In a patient with stable disease on anatomic imaging, SSTR PET may be helpful every 2 to 3 years, to ensure that there is no disease progression with lesions occult on CT or MRI.

Pitfalls in Somatostatin Receptor Positron Emission Tomography Interpretation

Recognizing the physiologic distribution of the radiopharmaceutical and potential false positives and false negatives is crucial for an accurate interpretation of the scan.

A common pitfall is the physiologic uptake in normal or hypertrophic pancreatic islet cells, which can demonstrate focal uptake, most commonly present in the uncinate process (see Fig. 5) but can also be seen elsewhere in the pancreas, such as the pancreatic tail.^{22,23} Generally, a higher degree of uptake is seen in NETs relative to the physiologic uptake in islet cells^{24–26} but standardized uptake values (SUVs) overlap and there is no clear cutoff. Imaging features that can help differentiate include the ill-defined margins of the physiologic uptake, the curvilinear appearance when located in the uncinate process,²⁷ and most importantly, the absence of corresponding lesion on multiphase contrast-enhanced anatomic imaging.

Another frequent pitfall is physiologic uptake in splenic tissue. Heterotopic intra-pancreatic accessory spleen (splenule) can mimic NET on CT or MRI. In fact, splenules can be found anywhere in the abdomen and can be misdiagnosed as metastatic lymph nodes or implants. It is important to recognize that SSTR PET is not an appropriate test to differentiate NET from a splenule, as both entities show intense uptake on this scan.²⁸ $^{99\text{m}}\text{Tc}$ -heat damaged red blood cells or $^{99\text{m}}\text{Tc}$ -sulfur colloid Single Photon

Table 3
Most appropriate indications for somatostatin receptor PET, based on the appropriate use criteria published by the Society of Nuclear Medicine and Molecular Imaging

Indication	Comments
Initial staging after histologic diagnosis of NETs	SSTR PET is superior to both conventional imaging (CI) and SSTR scintigraphy, making it the modality of choice for staging (see Figs. 1 and 5)
Localization of unknown primary tumor in patients with known metastatic disease	Even when metastatic, localization of the primary site is important to guide treatment. SSTR PET helps localize the primary in patients who are left with unknown primaries after initial workup (see Figs. 6 and 7)
Selection of patients for SSTR-targeted peptide receptor radionuclide therapy (PRRT)	Eligibility for PRRT is determined by translating the Krenning score to the maximal intensity projection image from SSTR PET
Staging of NETs before planned surgery	Cytoreduction or surgical debulking, although noncurative, helps improve survival for patients with metastatic disease predominantly to the liver and abdominal lymph nodes. SSTR PET allows evaluation of nonresectable extrahepatic disease (most commonly to bones), which when extensive, may reduce the benefits of cytoreduction
Evaluation of mass suggestive of NET but not amenable to endoscopic or percutaneous biopsy	For example, mesenteric mass or ileal lesion
Monitoring of disease seen predominantly on SSTR PET	Osseous lesions in particular are frequently occult on CT, making SSTR PET useful for routine follow-up (see Fig. 8)
Evaluation of patients with biochemical evidence and symptoms of NET but without evidence on anatomic imaging and prior histologic diagnosis of NET	Although the yield is low, SSTR PET is nonetheless cost-effective, as a negative scan could prevent further diagnostic workup
Restaging at time of clinical or biochemical progression, without evidence of progression on anatomic imaging	It is very important to keep in mind the superiority of SSTR PET to CI in such scenarios: A lesion seen for the first time on SSTR PET, and is occult on CI, remains of unknown chronicity, and does not indicate disease progression. Similarly, comparison between ^{64}Cu -DOTATATE and ^{68}Ga -DOTATATE PET requires careful consideration to differentiate between true new lesions vs better visualization of preexisting ones (see Fig. 14)
New indeterminate lesion on anatomic imaging, with unclear progression	SSTR PET may be useful both to verify that a new lesion is a NET (in case of uptake) or raise the suspicion of tumor dedifferentiation (in case of decreasing or low uptake)

(continued on next page)

Table 3 (continued)	
Indication	Comments
Restaging of patients post-PRRT	(added in the updated AUC in 2020) SSTR PET serves as a new baseline. Caution not to use changes in SUV as an indicator for disease response or progression. Appearance of new lesions or resolution of preexisting lesions should be used instead (see Figs. 9 and 10)

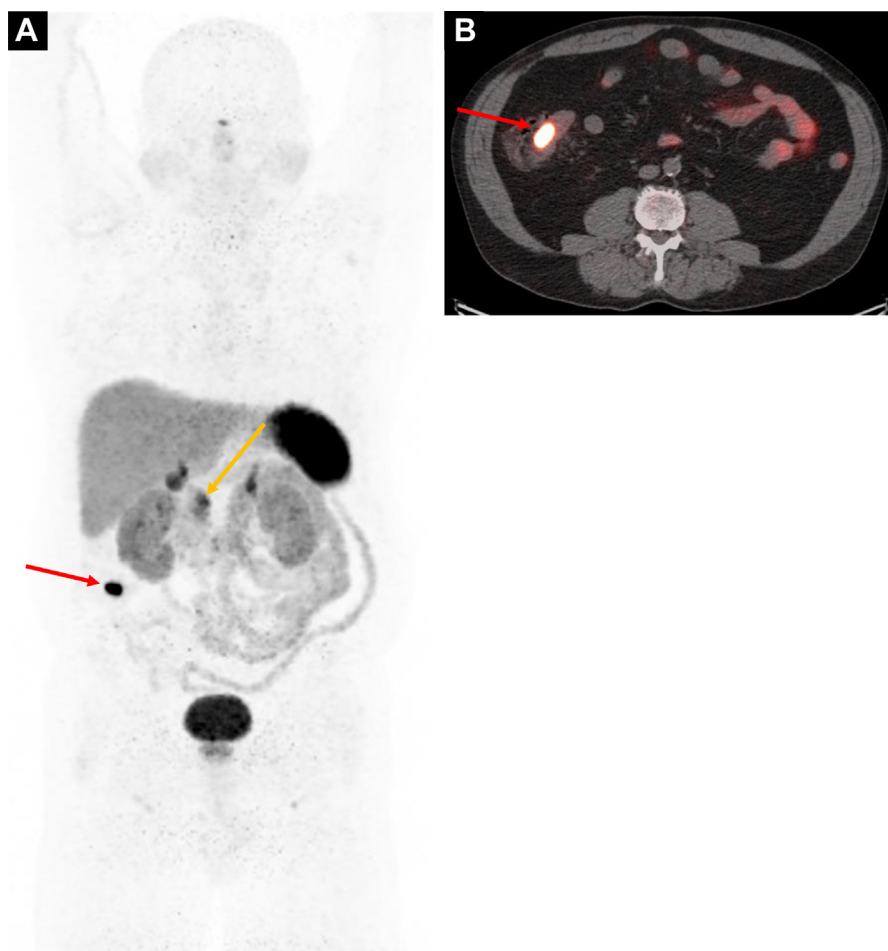


Fig. 5. Initial staging, patient with G1 ileal NET (Ki-67 < 3%). ⁶⁸Ga-DOTATATE PET/CT MIP image (A), and transaxial fused image (B) showing the primary tumor in the terminal ileum (*red arrow*) and no evidence of metastatic disease. Note the classic physiologic uptake in the uncinata process (*yellow arrow*).

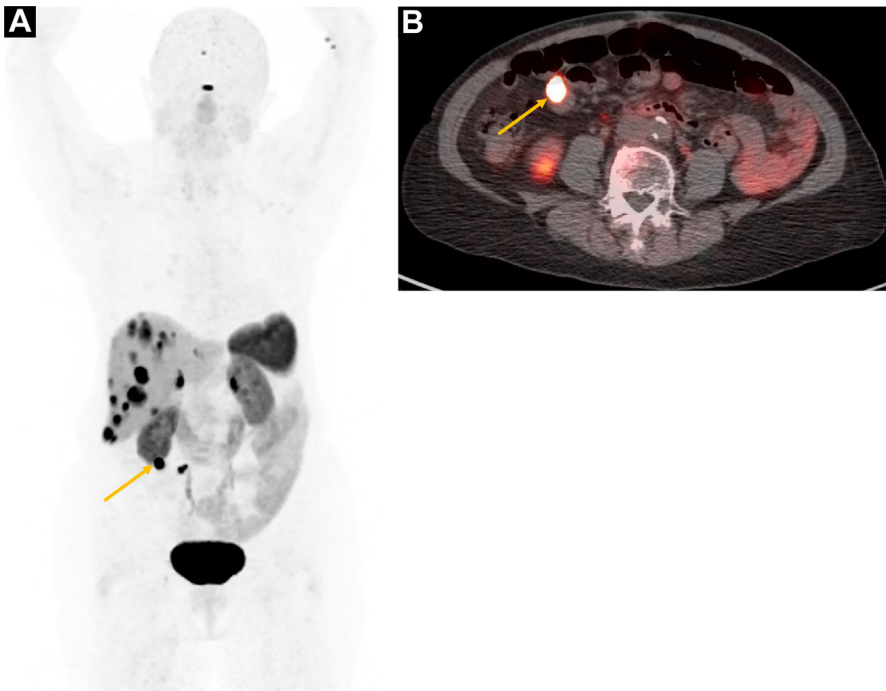


Fig. 6. Patient with hepatic lesions, biopsy proven G2 NET metastases with Ki-67 of 4%, of unknown primary. ^{64}Cu -DOTATATE PET MIP (A) and fused transaxial images (B) show intense uptake in the liver metastases, and localize the primary NET in the small bowel (arrow).

Emission Computed Tomography (SPECT)/CT can help differentiate because splenic tissue shows uptake with these 2 agents, whereas NETs do not (Fig. 11).^{29,30} Alternatively, MRI with superparamagnetic iron oxide (Ferumoxytol) can be used to differentiate, if available.³¹

Meningiomas demonstrate intense uptake and are frequently detected on SSTR PET as an incidental finding. Additional potential pitfalls include osteoblastic activity (degenerative bone changes, fibrous dysplasia, healing fractures, and vertebral hemangiomas) and inflammatory processes (reactive lymph nodes, infection); however, lower level of uptake can help differentiate these benign lesions from NETs (Fig. 12).²⁷

Comparison Between ^{64}Cu -DOTATATE and ^{68}Ga -DOTATATE/TOC

The physiologic distribution of ^{64}Cu -DOTATATE (Detectnet) is similar to that of ^{68}Ga -DOTATATE, except for less splenic uptake with ^{64}Cu -DOTATATE (Fig. 13). The longer half-life allows production in a central location and distribution to local PET centers,³² as well as more flexible uptake times, with no significant differences in the number of lesions detected between 60 minutes and 180 minutes postinjection scans.³³ The positron fraction of ^{64}Cu is only 18% (vs 89% for ^{68}Ga), which means fewer photon counts are collected per minute for the same injected activity, necessitating optimization of scanning parameters and protocols based on capabilities of various PET scanners. Table 4 shows comparison of physical properties of ^{64}Cu and ^{68}Ga pertinent to PET imaging.

^{64}Cu -DOTATATE PET imaging is highly accurate in detecting NETs. A prospective study with 63 subjects demonstrated 91% sensitivity, 97% specificity, 97% positive

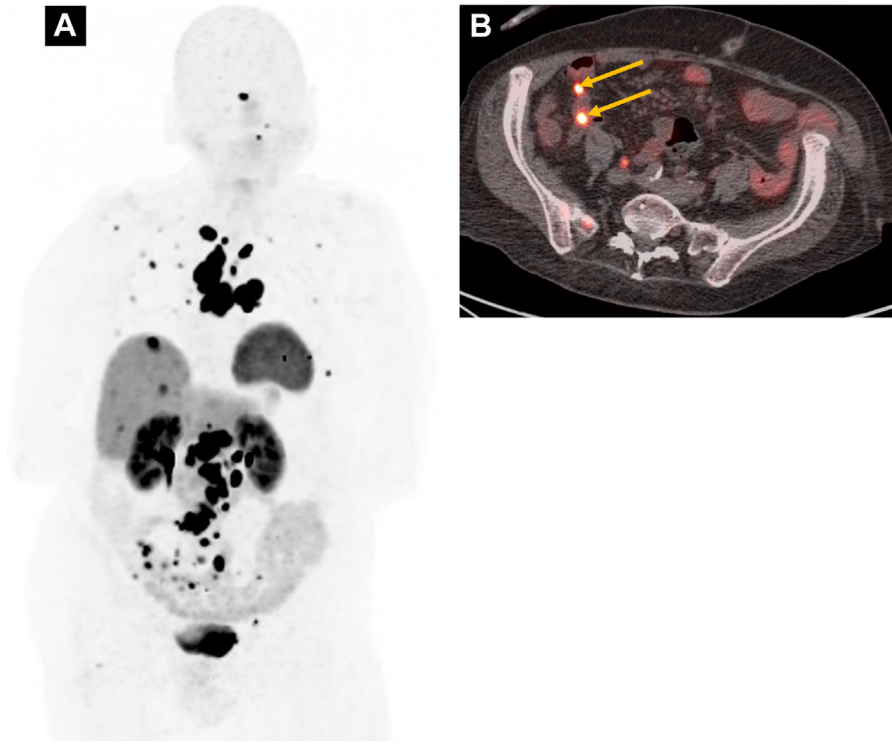


Fig. 7. ^{64}Cu -DOTATATE PET performed for localization of unknown primary in a patient with metastatic G1 NET, with liver, osseous, and lymph node metastases seen on MIP (A) Axial fused images (B) show multifocal small bowel foci of uptake (arrows) representing multifocal primaries, which can be seen in 30% to 40% of small bowel NETs.

predictive value, and 90% negative predictive value.³⁴ Excellent diagnostic performance of ^{64}Cu -DOTATATE is comparable to that of ^{68}Ga -DOTATATE/TOC. A head-to-head comparison study of ^{64}Cu -DOTATATE and ^{68}Ga -DOTATOC in 51 patients with NETs (mostly G1 and G2 gastroenteropancreatic [GEP] NETs) reported 100% sensitivity and 90% specificity for both agents, with no difference on a patient basis. However, significantly more true positive lesions were detected by ^{64}Cu -DOTATATE.³⁵ The higher rate of detection was mostly in small-sized lesions, presumably due to the shorter positron range of ^{64}Cu that provides better spatial resolution (Fig. 14, see Table 4).

In conclusion, ^{64}Cu -DOTATATE is a safe and high-quality radioligand for NET imaging, overall considered equivalent to ^{68}Ga -labelled agents; however, due to its unique physical properties, it requires optimization of imaging protocols and reconstruction parameters. It provides logistic advantages for PET centers without access to ^{68}Ga -labelled agents.

Fluorodeoxyglucose Positron Emission Tomography in the Imaging of Neuroendocrine Tumors

FDG PET uses a radiolabeled glucose analog that detects rapidly growing metabolically active tumors. GEP NETs demonstrate a “flip-flop” phenomenon in which low uptake on FDG PET and high uptake on SSTR imaging characterize low-grade NETs

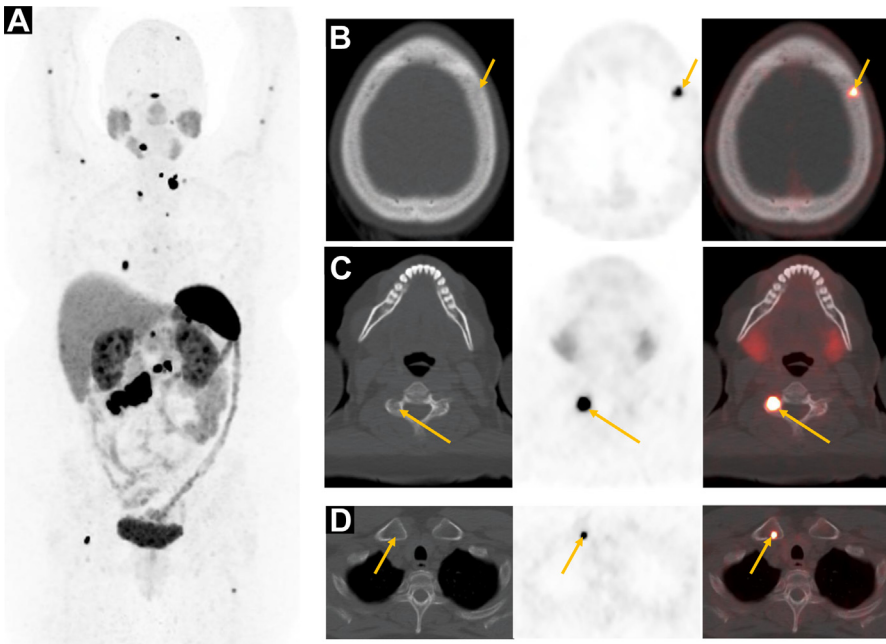


Fig. 8. Initial staging of patient with G1 small bowel NET (Ki-67 < 3%). ^{64}Cu -DOTATATE PET-CT MIP image (A) shows diffuse osseous metastases. Transaxial images (B–D) show most osseous metastases to be occult on CT (arrows).

(Fig. 15), whereas more aggressive NETs demonstrate high uptake on FDG PET and low uptake on SSTR imaging (Fig. 16).³⁶ Although most current North American consensus guidelines for the management of NETs do not mention the use of FDG PET, there is growing recognition that FDG PET should be considered in the evaluation

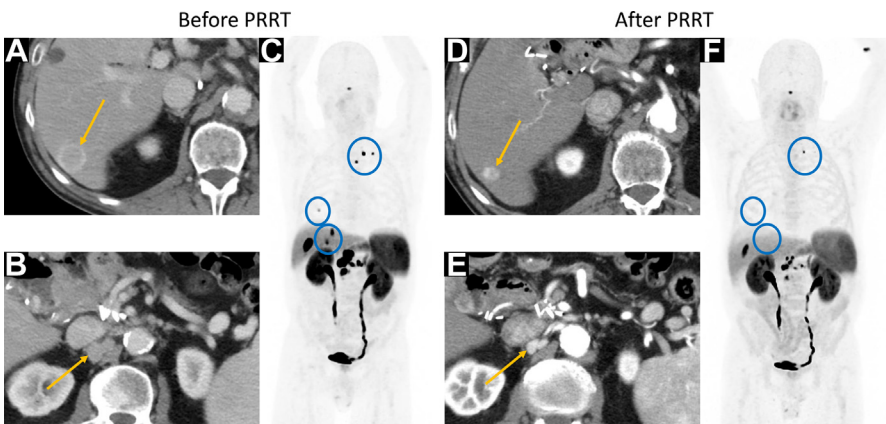


Fig. 9. Patient with G1 metastatic PNET treated with PRRT. Pretherapy contrast-enhanced abdominal CT (A, B) and ^{68}Ga -DOTATATE PET (C) show liver, retroperitoneal, and osseous metastases (arrows). Post-4 cycles of PRRT, decreased size of the liver metastases and retroperitoneal nodes on CT (D, E) (arrows), and resolution of several osseous and liver metastases on ^{64}Cu -DOTATATE PET (F) (blue circles). Findings consistent with disease response.

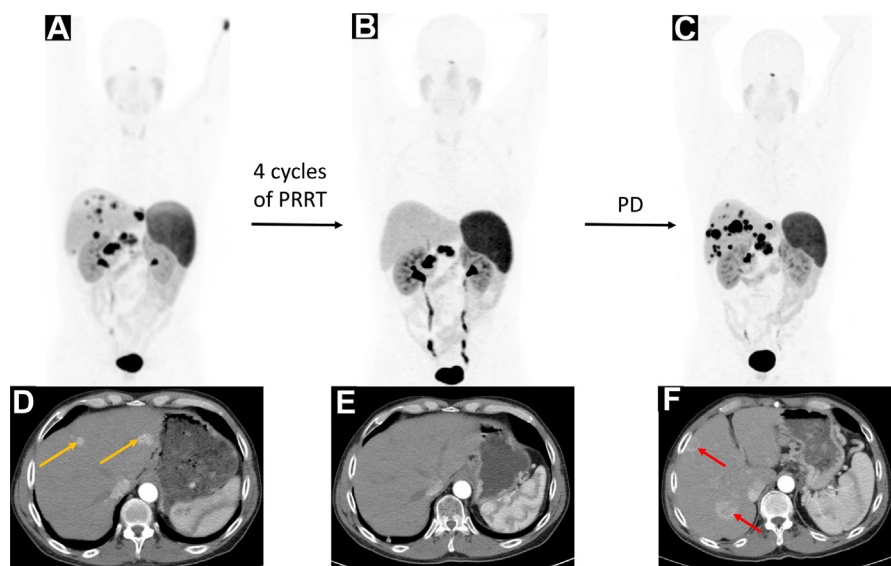


Fig. 10. Patient with G2 metastatic PNET treated with PRRT. ^{68}Ga -DOTATATE (A, B) and ^{64}Cu -DOTATATE (C) PET and corresponding arterial phase abdominal CT (D–F). Images post-4 cycles of PRRT (B, E) show disease response with resolution of the liver metastases (yellow arrows) compared with pretherapy scans (A, D). Twenty-three months later, restaging scans (C, F) show disease progression with multiple new liver lesions (red arrows).

of G3 tumors and more aggressive G2 tumors (Ki-67 index between 10% and 20%) as reflected in the recent European consensus guidelines.³⁷ In addition, there is mounting evidence that FDG PET may be a better prognosticating tool than the currently adopted histologic grading system based on the Ki-67 index for low-grade and intermediate-grade NETs (G1 and G2).^{38–42}

As discussed above, within the high-grade group (Ki-67 > 20%), there exists a “mixed grade” range of well-differentiated G3 tumors to poorly differentiated NECs.⁴³ This results in variability of uptake on FDG PET and SSTR imaging within this heterogeneous group. Poorly differentiated carcinomas would be expected to have less SSTR and high glucose metabolic activity, thus no or little uptake on SSTR imaging and high uptake on FDG PET. However, high-grade well-differentiated G3 NETs and more aggressive intermediate-grade G2 NETs can demonstrate uptake on both FDG PET and SSTR imaging (Fig. 17).^{38,39,41,44–46} In this group, uptake on SSTR imaging supports treatment with PRRT. However, FDG uptake in NETs

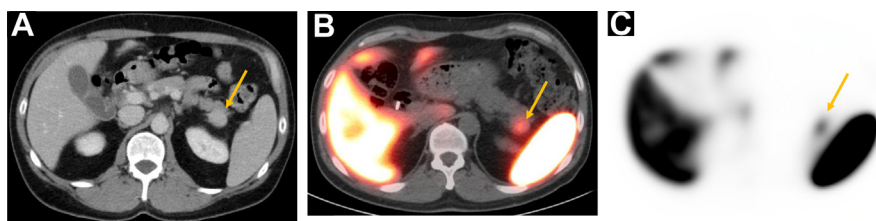


Fig. 11. Enhancing lesion in the pancreatic tail (arrow) on contrast-enhanced CT of the abdomen (A). $^{99\text{m}}\text{Tc}$ -heat denatured RBC scan, fused transaxial SPECT/CT (B) and SPECT only images (C) show uptake in the lesion confirming splenule.

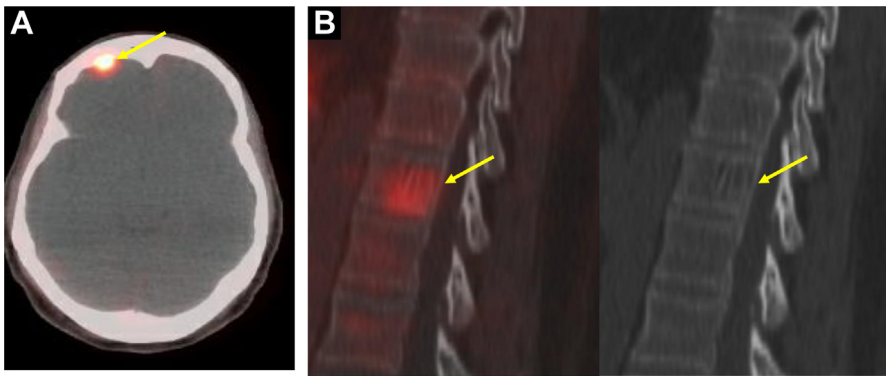


Fig. 12. (A) Arrow points to focal ^{68}Ga -DOTATATE uptake in the right frontal bone, corresponding to a benign meningioma. (B) Arrow points to mild focal ^{68}Ga -DOTATATE uptake in a vertebral body lesion, with a classic “corduroy” appearance on CT, consistent with a benign hemangioma.

demonstrating SSTR activity has been associated with less favorable overall survival (OS) and progression free survival (PFS) after PRRT than NETs with no FDG uptake.^{39,47} It has been recommended that patients with G3 and more aggressive G2 NETs undergo “complementary” FDG PET and SSTR imaging to determine if PRRT is an appropriate treatment choice and to gauge prognosis of response to PRRT.³⁷

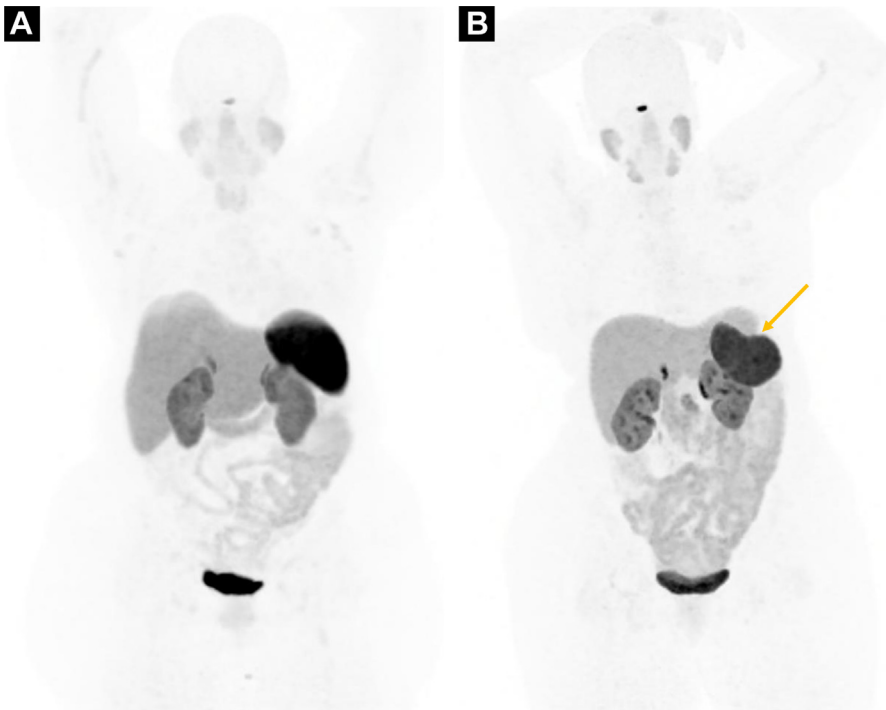


Fig. 13. Physiologic distribution of ^{68}Ga -DOTATATE (A) and ^{64}Cu -DOTATATE (B), with less intense splenic uptake (arrow) on the latter.

	^{64}Cu	^{68}Ga	Implication
Half-life	12.7 h	1.1 h	^{64}Cu allows for more flexible scanning time and for remote production in central locations with delivery to each site
Positron energy (maximum)	0.65 MeV	1.90 MeV	^{64}Cu offers higher spatial resolution, which improves detection of small lesions
Positron range (mean)	0.56 mm	3.50 mm	
Production	Cyclotron	Generator/Cyclotron	
Positron fraction	18%	89%	Low signal-to-noise ratio with ^{64}Cu can be overcome by scanning longer and using noise-reducing reconstruction algorithms

FDG PET has also been recommended in low-grade NETs with rapid progression or with disease seen on CT/MRI with negative SSTR imaging (Fig. 18).³⁷ Otherwise, utilization of FDG PET in this group is not routinely recommended due to the slow growth and low metabolic activity. These tumors demonstrate high uptake on SSTR imaging. However, studies have shown that 49% of patients with G1/G2 tumors (and even 21%–40% with G1 disease) can have FDG uptake, which is associated with a worse prognosis.^{38–40} This paradox may be explained by biopsy sampling error, tumor

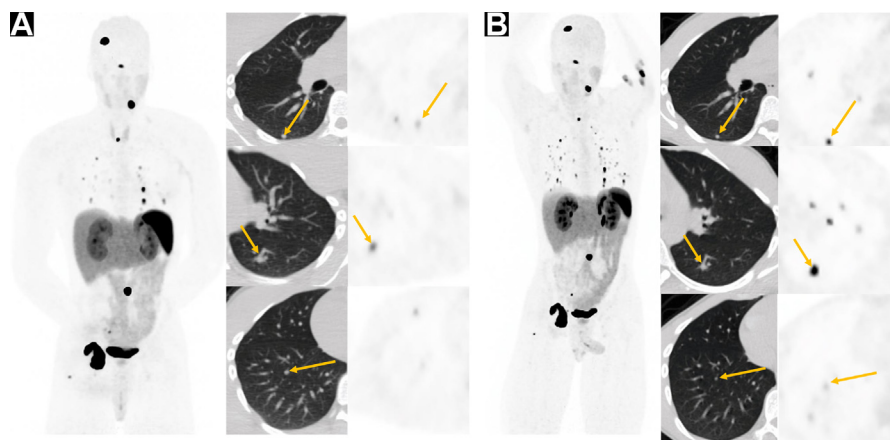


Fig. 14. We are using this case of metastatic paraganglioma to illustrate the importance of not relying solely on the degree of uptake to evaluate disease response post-PRRT, which in this case, might be at least partially related to difference in physical properties between ^{68}Ga and ^{64}Cu . Initial ^{68}Ga -DOTATATE PET/CT (A) and post-4 cycles of PRRT ^{64}Cu -DOTATATE PET/CT (B): Although more foci of uptake are seen in the lungs post-PRRT (B), the CT correlate shows all nodules to be stable or mildly decreased in size compared with (A), no new or enlarging nodules; findings consistent with overall stable disease. The better spatial resolution of ^{64}Cu can improve the detection of small lesions.

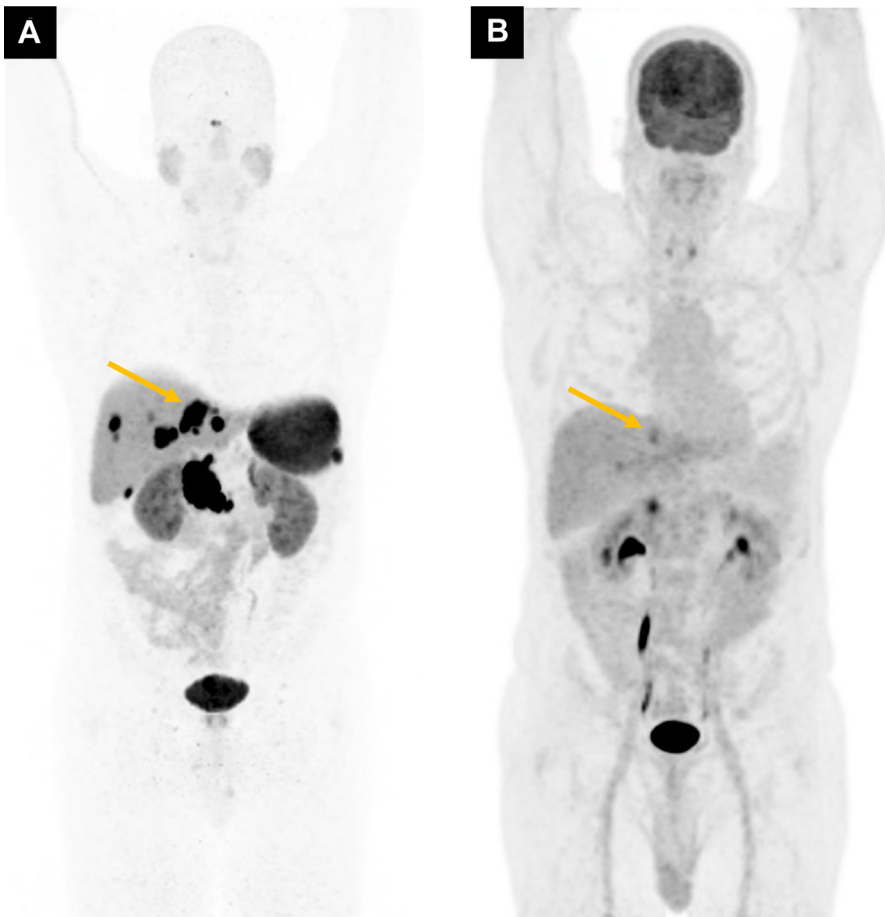


Fig. 15. G2 PNET (Ki-67 4%) metastatic to the liver (*arrows*), demonstrating high SSTR expression on ^{64}Cu -DOTATATE PET (A) and minimal uptake on ^{18}F -FDG PET (B). Studies performed 23 days apart.

heterogeneity, and Ki-67 grading observer intervariability during initial evaluation as well as tumor progression during the disease course.^{48,49} There may also be unknown tumor characteristics that could promote tumor aggressiveness. The clinical relevance of FDG uptake in these tumors has been demonstrated in a recent prospective 10-year follow-up study, which demonstrated a significantly longer 5-year OS (79% vs 35%) and PFS (49% vs 18%) in patients with negative FDG PET compared with positive FDG PET, also seen in a separate subanalysis of patients with G1 and G2 tumors.³⁹ This study also found that in the subset of patients who underwent PRRT, 93.5% were G1 or G2, and FDG-negative patients had longer OS.³⁹ This finding supports a recent large retrospective study of post-PRRT patients in which FDG uptake was an independent prognostic factor associated with decreased median OS.⁴⁷ Several studies suggest that FDG uptake may be a better prognostic marker for stratifying the metastatic potential and aggressiveness of low-grade and intermediate-grade NETs than the Ki-67 index.^{40,41,44,50}



Fig. 16. Well-differentiated G2 PNET metastatic to the liver (Ki-67 10%–15%) and lungs (*arrows*), demonstrating no significant SSTR expression on ^{64}Cu -DOTATATE PET (A) and increased uptake on ^{18}F -FDG PET (B). Studies performed 2 weeks apart.

Imaging Criteria for Selection for Peptide Receptor Radionuclide Therapy

PRRT with ^{177}Lu -DOTATATE (Lutathera™, Advanced Accelerator Applications USA, Inc., NJ 07041) was FDA approved for the treatment of progressive metastatic well-differentiated NETs in 2018. In general, ideal candidates are patients with progressing inoperable or metastatic well-differentiated NETs who show sufficient tumor uptake on SSTR imaging, which is defined as higher-than-liver uptake.¹⁵ Although the NETTER-1 trial (phase III trial of ^{177}Lu -DOTATATE plus long-acting octreotide versus high-dose long-acting octreotide in patients with midgut NETs),⁵¹ which led to the FDA approval of ^{177}Lu -DOTATATE, considered patients eligible for treatment based on highest tumor uptake equal to or higher than liver based on ^{111}In -pentetreotide imaging,⁵² it is acceptable to extrapolate this scale to SSTR PET (modified Krenning score, [Table 5](#)).⁵³ However, given the higher sensitivity of PET over planar or SPECT imaging, one should be cautious particularly for small lesions (<2 cm) because these lesions considered eligible per SSTR PET might have not shown uptake higher than liver on ^{111}In -pentetreotide scan.⁵⁴ In addition to the condition of a positive SSTR PET, patients should have sufficient bone marrow reserve, adequate kidney and liver function, good performance status, and expected survival longer than 3 to 6 months to be eligible for PRRT.⁵⁵ Selecting and sequencing treatments is a complex decision, and it must be based on a multidisciplinary team discussion and risk to benefit assessment of individual patients.⁵⁶

Response Assessment Postpeptide Receptor Radionuclide Therapy

Unlike the uptake on FDG PET, which reflects tumor metabolism correlating with aggressive disease and poor prognosis, the uptake on SSTR PET reflects SSTR

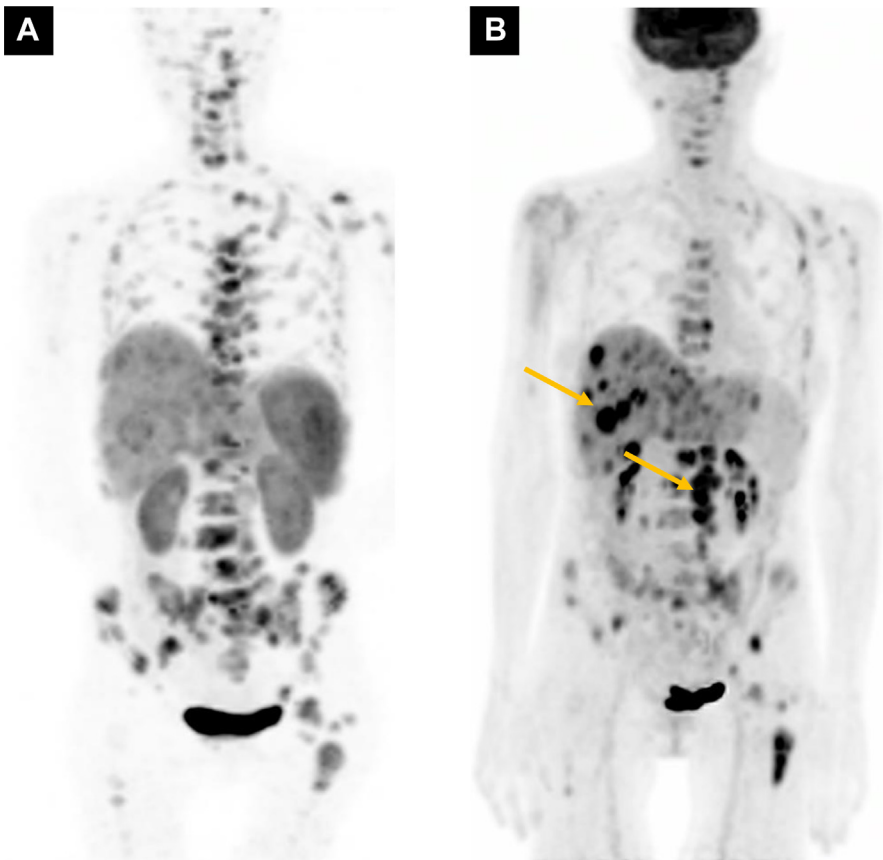


Fig. 17. Patient with metastatic G2 PNET (Ki-67 8%) demonstrating heterogeneous uptake on ^{68}Ga -DOTATATE PET (A) and ^{18}F -FDG PET (B). The bone lesions show heterogeneous uptake on both tracers; the liver and retroperitoneal nodes show uptake mostly with FDG (arrows).

density on the cell surface, which carries different implications. Studies have shown that changes in the degree of uptake, that is, SUVs in NETs after PRRT do not correlate with outcomes.^{57,58}

Huizing and colleagues⁵⁷ demonstrated in a retrospective analysis that the disease progression on anatomic imaging at 9 months post-PRRT indicates worse OS; however, they did not find an association between OS and the change in uptake on SSTR PET or chromogranin A levels. However, SSTR PET detected disease progression earlier than anatomic imaging, with new lesions only seen on SSTR PET but not on anatomic imaging at 3 months post-PRRT.

Tumor heterogeneity in metastatic NETs on SSTR PET has been shown to correlate with a worse prognosis and to outperform SUVs and Ki-67 as a prognostic marker.^{59–61} This heterogeneity constitutes an inherent limitation for conventional PET parameters because PRRT targets well-differentiated SSTR expressing clones, whereas sparing poorly differentiated ones.^{15,62}

Although imperfect for NETs due to their slow growth, based on current literature, morphologic evaluation using Response Evaluation Criteria In Solid Tumors (RECIST

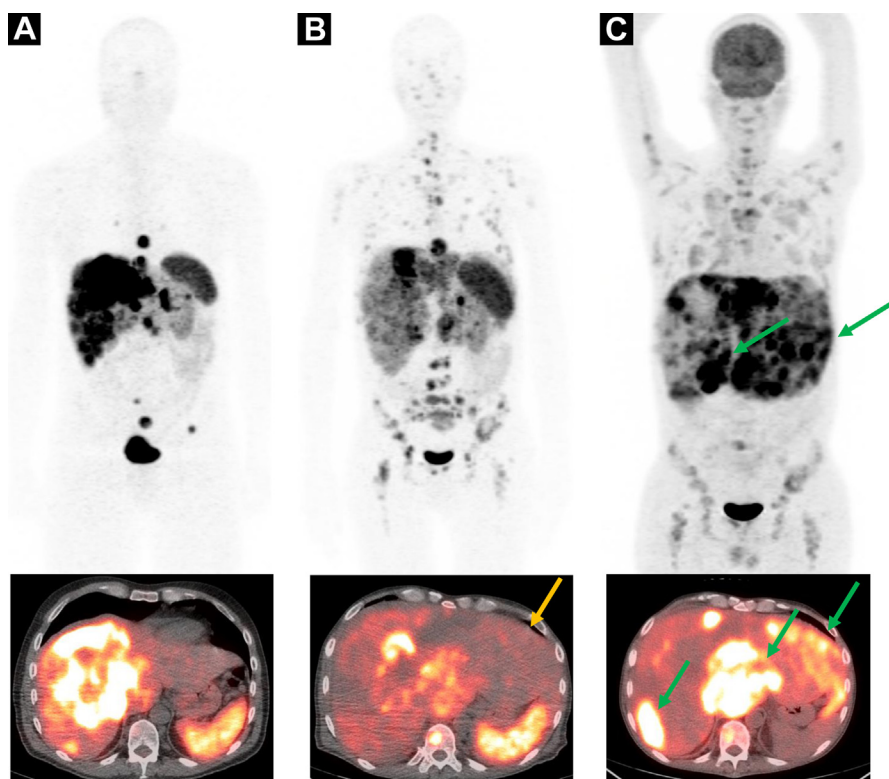


Fig. 18. Patient with metastatic well-differentiated G3 PNET. Initial (A) and 3 months follow-up (B) ^{68}Ga -DOTATATE MIP and fused transaxial PET/CT images show disease progression with new extensive bone metastases on (B); note the enlargement of the left hepatic lobe (yellow arrow) on (B) compared with (A) with no DOTATATE uptake, concerning for dedifferentiated/high-grade tumor, which prompted FDG PET. ^{18}F -FDG-PET/CT (C) shows increased uptake in the left hepatic lobe, in addition to multiple additional hypermetabolic liver metastases (green arrows), compatible with high-grade lesions.

1.1),⁶³ which are based on changes in size of target lesions on CT/MRI, remain the most established response assessment scheme so far. SSTR PET, however, can add valuable information in determining early disease progression by detecting new metastases occult on anatomic imaging^{57,58} and in establishing a new post-therapy baseline scan. The SNMMI AUC emphasize that changes in SUVs alone on post-PRRT SSTR PET do not indicate disease response or progression. Response should be assessed by the disappearance of known lesions or development of new ones (see Fig. 9).

Table 5
(Modified) Kenning score

0	No Uptake
1	Very low uptake
2	Uptake lower than or equal to liver
3	Uptake higher than liver
4	Very intense uptake or uptake higher than spleen

SUMMARY

In the last few years, SSTR PET imaging, mostly with ^{68}Ga -DOTATATE, has become the gold standard for imaging of well-differentiated NETs. SSTR PET is very useful in various clinical scenarios including but not limited to initial staging after histologic diagnosis of NETs, localizing unknown primary tumor in patients presenting with metastases, and selecting patients for PRRT. Recently, ^{64}Cu -DOTATATE was added to the list of FDA-approved radiopharmaceuticals for NET imaging. Longer half-life of ^{64}Cu expands imaging access by allowing long distance delivery and more flexible scanning windows. FDG PET complements SSTR PET, particularly for G3 and high G2 tumors. Increased FDG uptake is a significant prognostic factor implicating more aggressive disease and worse prognosis.

CLINICS CARE POINTS

- Anatomic imaging performed to evaluate NETs should include multiphase imaging of the abdomen.
- SSTR PET is the modality of choice for functional imaging of well-differentiated NETs.
- FDG PET is complimentary to SSTR PET, particularly for imaging of high grade NETs.

ACKNOWLEDGMENTS

The search tool developed by Li and colleagues⁶⁴ was invaluable in finding illustrative cases for this publication.

DISCLOSURE

The authors have nothing to disclose.

REFERENCES

1. Shah MH, Goldner WS, Benson AB, et al. Neuroendocrine and Adrenal Tumors, Version 2.2021, NCCN Clinical Practice Guidelines in Oncology. *J Natl Compr Canc Netw* 2021;19(7):839–68.
2. Dasari A, Shen C, Halperin D, et al. Trends in the incidence, prevalence, and survival outcomes in patients with neuroendocrine tumors in the United States. *JAMA Oncol* 2017;3(10):1335–42.
3. Rindi G, Klimstra DS, Abedi-Ardekani B, et al. A common classification framework for neuroendocrine neoplasms: an International Agency for Research on Cancer (IARC) and World Health Organization (WHO) expert consensus proposal. *Mod Pathol* Dec 2018;31(12):1770–86.
4. Nagtegaal ID, Odze RD, Klimstra D, et al. The 2019 WHO classification of tumours of the digestive system. *Histopathology* 2020;76(2):182–8.
5. Maxwell JE, O'Dorisio TM, Howe JR. Biochemical diagnosis and preoperative imaging of gastroenteropancreatic neuroendocrine tumors. *Surg Oncol Clin N Am* 2016;25(1):171–94.
6. Sahani DV, Bonaffini PA, Fernández-Del Castillo C, et al. Gastroenteropancreatic neuroendocrine tumors: role of imaging in diagnosis and management. *Radiology* 2013;266(1):38–61.

7. Bushnell DL, Baum RP. Standard imaging techniques for neuroendocrine tumors. *Endocrinol Metab Clin North Am* 2011;40(1):153–62, ix.
8. Kuo JH, Lee JA, Chabot JA. Nonfunctional pancreatic neuroendocrine tumors. *Surg Clin North Am* 2014;94(3):689–708.
9. Dahdaleh FS, Lorenzen A, Rajput M, et al. The value of preoperative imaging in small bowel neuroendocrine tumors. *Ann Surg Oncol* 2013;20(6):1912–7.
10. Dromain C, de Baere T, Lumbroso J, et al. Detection of liver metastases from endocrine tumors: a prospective comparison of somatostatin receptor scintigraphy, computed tomography, and magnetic resonance imaging. *J Clin Oncol* 2005;23(1):70–8.
11. Yu R, Wachsman A. Imaging of neuroendocrine tumors: indications, interpretations, limits, and pitfalls. *Endocrinol Metab Clin North Am* 2017;46(3):795–814.
12. Shimada K, Isoda H, Hirokawa Y, et al. Comparison of gadolinium-EOB-DTPA-enhanced and diffusion-weighted liver MRI for detection of small hepatic metastases. *Eur Radiol* 2010;20(11):2690–8.
13. Ba-Ssalamah A, Uffmann M, Saini S, et al. Clinical value of MRI liver-specific contrast agents: a tailored examination for a confident non-invasive diagnosis of focal liver lesions. *Eur Radiol* 2009;19(2):342–57.
14. Giesel FL, Kratochwil C, Mehndiratta A, et al. Comparison of neuroendocrine tumor detection and characterization using DOTATOC-PET in correlation with contrast enhanced CT and delayed contrast enhanced MRI. *Eur J Radiol* 2012; 81(10):2820–5.
15. Park S, Parihar AS, Bodei L, et al. Somatostatin Receptor Imaging and Theranostics: Current Practice and Future Prospects. *J Nucl Med* 2021;62(10):1323–9.
16. Reubi JC. Peptide receptor expression in GEP-NET. *Virchows Arch* 2007; 451(Suppl 1):S47–50.
17. NETSPOT (kit for the preparation of gallium Ga-68 DOTATATE injection). Available at: https://www.accessdata.fda.gov/drugsatfda_docs/nda/2016/208547Orig1s000TOC.cfm. Accessed November 27, 2021.
18. Drug approval package: Gallium DOTATOC Ga-68. 2021. Available at: https://www.accessdata.fda.gov/drugsatfda_docs/nda/2019/210828Orig1s000TOC.cfm. Accessed November 27, 2021.
19. Cu-64 DOTATATE (Detectnet™) full prescribing information. Available at: https://www.accessdata.fda.gov/drugsatfda_docs/label/2020/213227s000lbl.pdf. Accessed November 27, 2021.
20. Hope TA, Bergsland EK, Bozkurt MF, et al. Appropriate use criteria for somatostatin receptor PET imaging in neuroendocrine tumors. *J Nucl Med* 2018;59(1): 66–74.
21. Hope TA. Updates to the appropriate-use criteria for somatostatin receptor PET. *J Nucl Med* 2020;61(12):1764.
22. Jacobsson H, Larsson P, Jonsson C, et al. Normal uptake of 68Ga-DOTA-TOC by the pancreas uncinate process mimicking malignancy at somatostatin receptor PET. *Clin Nucl Med* 2012;37(4):362–5.
23. Delbeke D, Newman G, Deppen S, et al. 68Ga-DOTATATE: significance of uptake in the tail of the pancreas in patients without lesions. *Clin Nucl Med* 2019;44(11): 851–4.
24. Kroiss A, Putzer D, Decristoforo C, et al. 68Ga-DOTA-TOC uptake in neuroendocrine tumour and healthy tissue: differentiation of physiological uptake and pathological processes in PET/CT. *Eur J Nucl Med Mol Imaging* 2013;40(4):514–23.

25. Al-Ibraheem A, Bundschuh RA, Notni J, et al. Focal uptake of 68Ga-DOTATOC in the pancreas: pathological or physiological correlate in patients with neuroendocrine tumours? *Eur J Nucl Med Mol Imaging* 2011;38(11):2005–13.
26. Krausz Y, Rubinstein R, Appelbaum L, et al. Ga-68 DOTA-NOC uptake in the pancreas: pathological and physiological patterns. *Clin Nucl Med* 2012;37(1):57–62.
27. Hofman MS, Lau WF, Hicks RJ. Somatostatin receptor imaging with 68Ga DOTA-TATE PET/CT: clinical utility, normal patterns, pearls, and pitfalls in interpretation. *Radiographics* 2015;35(2):500–16.
28. Lancellotti F, Sacco L, Cerasari S, et al. Intrapancreatic accessory spleen false positive to 68Ga-Dotatoc: case report and literature review. *World J Surg Oncol* 2019;17(1):117.
29. Shah M, McClelland A, Moadel R, et al. Splenule disguised as pancreatic mass: elucidated with SPECT liver-spleen scintigraphy. *Clin Nucl Med* 2014;39(9):e405–6.
30. Belkhir SM, Archambaud F, Prigent A, et al. Intrapancreatic accessory spleen diagnosed on radionuclide imaging. *Clin Nucl Med* 2009;34(9):642–4.
31. Muehler MR, Rendell VR, Bergmann LL, et al. Ferumoxytol-enhanced MR imaging for differentiating intrapancreatic splenules from other tumors. *Abdom Radiol (Ny)* 2021;46(5):2003–13.
32. Pfeifer A, Knigge U, Binderup T, et al. 64Cu-DOTATATE PET for neuroendocrine tumors: a prospective head-to-head comparison with 111In-DTPA-Octreotide in 112 Patients. *J Nucl Med* 2015;56(6):847–54.
33. Loft M, Carlsen EA, Johnbeck CB, et al. (64)Cu-DOTATATE PET in Patients with neuroendocrine neoplasms: prospective, head-to-head comparison of imaging at 1 hour and 3 hours After Injection. *J Nucl Med* 2021;62(1):73–80.
34. Delpassand ES, Ranganathan D, Wagh N, et al. (64)Cu-DOTATATE PET/CT for imaging patients with known or suspected somatostatin receptor-positive neuroendocrine tumors: results of the first U.S. prospective, reader-masked clinical trial. *J Nucl Med* 2020;61(6):890–6.
35. Johnbeck CB, Knigge U, Loft A, et al. Head-to-Head Comparison of (64)Cu-DOTATATE and (68)Ga-DOTATOC PET/CT: A Prospective Study of 59 Patients with Neuroendocrine Tumors. *J Nucl Med* 2017;58(3):451–7.
36. Kayani I, Bomanji JB, Groves A, et al. Functional imaging of neuroendocrine tumors with combined PET/CT using 68Ga-DOTATATE (DOTA-DPhe1,Tyr3-octreotate) and 18F-FDG. *Cancer* 2008;112(11):2447–55.
37. Ambrosini V, Kunikowska J, Baudin E, et al. Consensus on molecular imaging and theranostics in neuroendocrine neoplasms. *Eur J Cancer* Mar 2021;146:56–73.
38. Bahri H, Laurence L, Edeline J, et al. High prognostic value of 18F-FDG PET for metastatic gastroenteropancreatic neuroendocrine tumors: a long-term evaluation. *J Nucl Med* 2014;55(11):1786–90.
39. Binderup T, Knigge U, Johnbeck CB, et al. (18)F-FDG PET is Superior to WHO Grading as a Prognostic Tool in Neuroendocrine Neoplasms and Useful in Guiding PRRT: A Prospective 10-Year Follow-up Study. *J Nucl Med* 2021;62(6):808–15.
40. Binderup T, Knigge U, Loft A, et al. 18F-fluorodeoxyglucose positron emission tomography predicts survival of patients with neuroendocrine tumors. *Clin Cancer Res* 2010;16(3):978–85.
41. Ezziddin S, Adler L, Sabet A, et al. Prognostic stratification of metastatic gastroenteropancreatic neuroendocrine neoplasms by 18F-FDG PET: feasibility of a metabolic grading system. *J Nucl Med* 2014;55(8):1260–6.

42. Rinzivillo M, Partelli S, Prosperi D, et al. Clinical Usefulness of (18)F-Fluorodeoxyglucose Positron Emission Tomography in the Diagnostic Algorithm of Advanced Entero-Pancreatic Neuroendocrine Neoplasms. *Oncologist* 2018; 23(2):186–92.
43. Tang LH, Untch BR, Reidy DL, et al. Well-differentiated neuroendocrine tumors with a morphologically apparent high-grade component: a pathway distinct from poorly differentiated neuroendocrine carcinomas. *Clin Cancer Res* 2016; 22(4):1011–7.
44. Binderup T, Knigge U, Loft A, et al. Functional imaging of neuroendocrine tumors: a head-to-head comparison of somatostatin receptor scintigraphy, 123I-MIBG scintigraphy, and 18F-FDG PET. *J Nucl Med* 2010;51(5):704–12.
45. Deroose CM, Hindie E, Kebebew E, et al. Molecular Imaging of Gastroenteropancreatic Neuroendocrine Tumors: Current Status and Future Directions. *J Nucl Med* 2016;57(12):1949–56.
46. Has Simsek D, Kuyumcu S, Turkmen C, et al. Can complementary 68Ga-DOTA-TATE and 18F-FDG PET/CT establish the missing link between histopathology and therapeutic approach in gastroenteropancreatic neuroendocrine tumors? *J Nucl Med* 2014;55(11):1811–7.
47. Zhang J, Liu Q, Singh A, et al. Prognostic Value of (18)F-FDG PET/CT in a Large Cohort of Patients with Advanced Metastatic Neuroendocrine Neoplasms Treated with Peptide Receptor Radionuclide Therapy. *J Nucl Med* 2020;61(11):1560–9.
48. Polley MY, Leung SC, McShane LM, et al. An international Ki67 reproducibility study. *J Natl Cancer Inst* 2013;105(24):1897–906.
49. Singh S, Hallet J, Rowsell C, et al. Variability of Ki67 labeling index in multiple neuroendocrine tumors specimens over the course of the disease. *Eur J Surg Oncol* 2014;40(11):1517–22.
50. Garin E, Le Jeune F, Devillers A, et al. Predictive value of 18F-FDG PET and somatostatin receptor scintigraphy in patients with metastatic endocrine tumors. *J Nucl Med* 2009;50(6):858–64.
51. Strosberg J, El-Haddad G, Wolin E, et al. Phase 3 Trial of (177)Lu-Dotatate for Midgut Neuroendocrine Tumors. *N Engl J Med* 2017;376(2):125–35.
52. Krenning EP, Valkema R, Kooij PP, et al. Scintigraphy and radionuclide therapy with [indium-111-labelled-diethyl triamine penta-acetic acid-D-Phe1]-octreotide. *Ital J Gastroenterol Hepatol* 1999;31(Suppl 2):S219–23.
53. Werner RA, Solnes LB, Javadi MS, et al. SSTR-RADS Version 1.0 as a Reporting System for SSTR PET Imaging and Selection of Potential PRRT Candidates: A Proposed Standardization Framework. *J Nucl Med* Jul 2018;59(7):1085–91.
54. Hope TA, Calais J, Zhang L, et al. (111)In-Pentetreotide Scintigraphy Versus (68)Ga-DOTATATE PET: Impact on Krenning Scores and Effect of Tumor Burden. *J Nucl Med* Sep 2019;60(9):1266–9.
55. Hicks RJ, Kwekkeboom DJ, Krenning E, et al. ENETS consensus guidelines for the standards of care in neuroendocrine neoplasia: peptide receptor radionuclide therapy with radiolabeled somatostatin analogues. *Neuroendocrinology* 2017;105(3):295–309.
56. Hope TA, Bodei L, Chan JA, et al. NANETS/SNMMI Consensus Statement on Patient Selection and Appropriate Use of (177)Lu-DOTATATE Peptide Receptor Radionuclide Therapy. *J Nucl Med* 2020;61(2):222–7.
57. Huizing DMV, Aalbersberg EA, Versleijen MWJ, et al. Early response assessment and prediction of overall survival after peptide receptor radionuclide therapy. *Cancer Imaging* 2020;20(1):57.

58. Gabriel M, Oberauer A, Dobrozemsky G, et al. 68Ga-DOTA-Tyr3-octreotide PET for assessing response to somatostatin-receptor-mediated radionuclide therapy. *J Nucl Med* 2009;50(9):1427–34.
59. Werner RA, Ilhan H, Lehner S, et al. Pre-therapy somatostatin receptor-based heterogeneity predicts overall survival in pancreatic neuroendocrine tumor patients undergoing peptide receptor radionuclide therapy. *Mol Imaging Biol* 2019;21(3):582–90.
60. Werner RA, Lapa C, Ilhan H, et al. Survival prediction in patients undergoing radionuclide therapy based on intratumoral somatostatin-receptor heterogeneity. *Oncotarget* 2017;8(4):7039–49.
61. Graf J, Pape UF, Jann H, et al. Prognostic Significance of somatostatin receptor heterogeneity in progressive neuroendocrine tumor treated with Lu-177 DOTA-TOC or Lu-177 DOTATATE. *Eur J Nucl Med Mol Imaging* 2020;47(4):881–94.
62. Roll W, Weckesser M, Seifert R, et al. Imaging and liquid biopsy in the prediction and evaluation of response to PRRT in neuroendocrine tumors: implications for patient management. *Eur J Nucl Med Mol Imaging* 2021;48(12):4016–27.
63. Eisenhauer EA, Therasse P, Bogaerts J, et al. New response evaluation criteria in solid tumours: revised RECIST guideline (version 1.1). *Eur J Cancer* 2009;45(2):228–47.
64. Li N, Maresh G, Cretcher M, et al., A modern non-SQL approach to radiology-centric search engine design with clinical validation, 2020, arXiv preprint arXiv:2007.02124.